ADVANCING EARTH AND SPACE SCIENCES

JGR Atmospheres

RESEARCH ARTICLE
10.1029/2024JD043183

Special Collection:
Chemistry and Climate Impacts of the Asian Summer Monsoon

Springtime UTLS Ozone Variability in East Asia: Insights From 16 Years of IASI Observations (2008–2023)

Chiyoung Kim[1], Joowan Kim[2], Jae-Heung Park[3], Ja-Ho Koo[4], Kyung-Hwan Kwak[5], Anne Boynard[6,7], Laura L. Pan[8], Cathy Clerbaux[6,9], Daniel Hurtmans[9], Pierre-François Coheur[9], and Sang Seo Park[1]

[1]Department of Civil, Urban, Earth, and Environmental Engineering, Ulsan National Institute of Science and Technology (UNIST), Ulsan, South Korea, [2]Department of Atmospheric Sciences, Kongju National University, Gongju, South Korea, [3]School of Earth and Environmental Sciences, Seoul National University, Seoul, South Korea, [4]Department of Atmospheric Sciences, Yonsei University, Seoul, South Korea, [5]School of Natural Resources and Environmental Science, Kangwon National University, Chuncheon, South Korea, [6]LATMOS/IPSL, Sorbonne Université, UVSQ, CNRS, Paris, France, [7]SPASCIA, Ramonville-Saint-Agne, France, [8]Atmospheric Chemistry Observations & Modeling, NSF National Center for Atmospheric Research, Boulder, CO, USA, [9]Spectroscopy, Quantum Chemistry and Atmospheric Remote Sensing (SQUARES), Université libre de Bruxelles (ULB), Brussels, Belgium

Key Points:

- The ozone variability in the upper troposphere and lower stratosphere over East Asia was analyzed by the Infrared Atmospheric Sounding Interferometer
- More than half of the variance in upper troposphere and lower stratosphere ozone revealed strong positive correlations in regions influenced by the East Asian jet stream

Supporting Information:

Supporting Information may be found in the online version of this article.

Correspondence to:

S. S. Park,
sangseopark@unist.ac.kr

Citation:

Kim, C., Kim, J., Park, J.-H., Koo, J.-H., Kwak, K.-H., Boynard, A., et al. (2025). Springtime UTLS ozone variability in East Asia: Insights from 16 years of IASI observations (2008–2023). *Journal of Geophysical Research: Atmospheres*, *130*, e2024JD043183. https://doi.org/10.1029/2024JD043183

Received 4 JAN 2025
Accepted 11 JUN 2025

Author Contributions:

Conceptualization: Kyung-Hwan Kwak, Sang Seo Park
Data curation: Anne Boynard, Laura L. Pan, Cathy Clerbaux, Daniel Hurtmans, Pierre-François Coheur
Formal analysis: Chiyoung Kim, Joowan Kim, Jae-Heung Park, Sang Seo Park
Funding acquisition: Ja-Ho Koo

Abstract We investigated the springtime variability of ozone in the upper troposphere and lower stratosphere (UTLS) over East Asia using data from the Infrared Atmospheric Sounding Interferometer (IASI) onboard the Metop satellite series (Metop-A, Metop-B, and Metop-C), complemented with ozonesonde observations and MERRA-2 reanalysis data. The accuracy of the IASI ozone profiles was confirmed through validation against ozonesonde measurements, demonstrating their reliability for monitoring UTLS ozone dynamics. An empirical orthogonal function analysis revealed that the first principal component explained more than half of the variance in UTLS ozone during springtime, with strong positive correlations in regions influenced by the East Asian jet stream (EAJS). The analysis showed that the strengthening of the jet stream was associated with increased ozone concentrations, likely driven by enhanced baroclinic wave activity and stratospheric intrusion. Moreover, the intensification of the EAJS was associated with strengthening of the local Hadley Cells and the meridional temperature gradient over the upstream region even during springtime.

Plain Language Summary Ozone in the atmosphere plays an important role in air quality and climate. In this study, we investigated how ozone levels change during springtime over East Asia using satellite observations and reanalysis data. We found that most of the ozone variability occurs in the upper troposphere and lower stratosphere, where the jet stream has a strong influence. More than half of the ozone variability in this region can be linked to changes in the jet stream. When the jet stream strengthens, ozone levels increase in the upper atmosphere because more ozone-rich air from the stratosphere moves down into the troposphere. Additionally, a stronger jet stream is linked to changes in large-scale circulation patterns and temperature differences between northern and southern regions. Our findings highlight the important role of atmospheric circulation in controlling ozone levels over East Asia, even during the spring season.

1. Introduction

Ozone is an important atmospheric component that contributes to the radiative balance in the atmosphere (Manabe & Möller, 1961). Variation in stratospheric ozone can modify hemispheric-scale temperature and precipitation patterns, thereby influencing atmospheric circulation through both radiative and dynamical processes (Jeong et al., 2021; Kang et al., 2011; Son et al., 2009). The representation of stratospheric ozone in climate models is therefore crucial to accurately estimate climate sensitivity (Nowack et al., 2015). Stratospheric ozone can be transported into the troposphere through a process known as stratospheric intrusion, which most commonly occurs at mid-latitudes and is associated with tropopause folding in the upper troposphere and lower stratosphere (UTLS) (Akritidis et al., 2021; Gettelman et al., 2011; Holton et al., 1995; Škerlak et al., 2014). Stratospheric ozone intrusions predominantly occur near the jet stream core, where jet-frontal zone dynamics play a key role in facilitating vertical mixing across the tropopause (Shapiro, 1980). Over East Asia, several studies have highlighted the role of the jet stream in modulating tropospheric ozone through such intrusions. For instance, Austin and Midgley (1994) demonstrated that the climatological jet stream core over Japan could significantly influence tropospheric ozone levels through the intrusion process during winter and spring. Moreover, Hwang et al. (2007)

Methodology: Chiyoung Kim, Joowan Kim, Jae-Heung Park, Sang Seo Park
Project administration: Ja-Ho Koo, Sang Seo Park
Resources: Sang Seo Park
Validation: Chiyoung Kim, Anne Boynard, Cathy Clerbaux, Daniel Hurtmans, Pierre-François Coheur, Sang Seo Park
Visualization: Chiyoung Kim
Writing – original draft: Chiyoung Kim
Writing – review & editing: Joowan Kim, Jae-Heung Park, Ja-Ho Koo, Kyung-Hwan Kwak, Anne Boynard, Laura L. Pan, Sang Seo Park

found that the occurrence of a secondary ozone peak in Pohang was strongly correlated with strong zonal wind speeds near the jet stream based on a 10-year record of ozonesonde data. Park et al. (2012) further confirmed that this secondary ozone peak was associated with the deepening of troughs in the upper troposphere and its occurrence was also correlated with an increase in total ozone. Despite these insights, the detailed three-dimensional structures and dynamic processes governing the coupling between the East Asian jet stream and ozone variability in the UTLS remain insufficiently understood.

Recently, significant increases in surface and tropospheric ozone have been observed despite emissions control policies in East Asia (Lee et al., 2021, 2022). In addition, background ozone levels in East Asia remain high at 55 ppb, even under a scenario with zero anthropogenic emissions (Colombi et al., 2023). The cause of this phenomenon remains unknown and the underlying mechanisms driving the general increase in tropospheric ozone over East Asia are also not fully understood, highlighting the need for further investigations. Although several processes have been proposed using model simulations, there is a need for observational studies over East Asia to substantiate the suggested mechanisms (e.g., Pan et al., 2024).

Tropospheric ozone concentrations are governed not only by emissions and chemical processes but also by large-scale climate variability. In particular, the El Niño-Southern Oscillation (ENSO) has emerged as a key modulator of ozone variability across different regions and seasons. Over East Asia, tropospheric column ozone has been observed to increase 4-5 months after La Niña events, a response attributed to enhanced cyclonic circulation over the western North Pacific, increased northerly subsidence, and reduced convection (Wie et al., 2021). Similarly, in southern China, an increase in summertime surface ozone has been linked to weakened southerly winds during El Niño years (Yang et al., 2022). Jeong et al. (2023) further reported that ENSO significantly influences tropospheric ozone concentrations across East Asia during both spring and summer. Beyond the East Asian domain, Lin et al. (2015), based on model simulations, showed that springtime high-ozone events in the western United States during spring are linked to ENSO-induced variations in the polar jet meandering, suggesting a hemispheric-scale influence of climate variability on ozone transport. These findings collectively underscore the importance of understanding how interannual climate modes shape ozone distributions, particularly in regions where background levels are persistently elevated.

Given the crucial role of UTLS ozone transport and stratosphere-troposphere exchange (STE) in explaining these trends, a comprehensive analysis requires reliable three-dimensional observational data. To achieve this, we utilized infrared satellite remote sensing, which provides vertical profiles of atmospheric composition. Among the available thermal infrared (TIR) instruments, we utilized the Infrared Atmospheric Sounding Interferometer (IASI), which was designed to balance the requirements for high spatial coverage with the need for accuracy and detailed vertical information (Clerbaux et al., 2009). This study aims to advance our understanding of the UTLS ozone variabilities in East Asia using TIR information. This method has not been extensively applied in previous studies and could therefore provide useful new information regarding ozone variation in the East Asia region. In addition, the large-scale atmospheric conditions associated with UTLS ozone were examined connecting the behavior of the jet stream and UTLS ozone variability. We focused on the primary factors influencing the variability of UTLS ozone in East Asia.

2. Data and Methods

2.1. IASI Ozone Profiles

The IASI is a nadir-viewing spectrometer (Clerbaux et al., 2009, 2015), and was launched on the Metop-A (October 2006), Metop-B (September 2012), and Metop-C (November 2018) satellites. Since 2007, the IASI instruments have monitored atmospheric composition, ensuring consistent long-term observations. IASI measures radiance spectra in the thermal infrared, between 645 and 2,760 cm^{-1} with twice-daily coverage. We used IASI ozone products retrieved using Fast Optimal Retrievals on Layers for IASI (FORLI) (Hurtmans et al., 2012) based on the optimal estimation method (OEM) (Rodgers, 2000). An a priori variance-covariance matrix was constructed with ozone climatology by McPeters et al. (2007). The EUMETSAT Level 2 temperature and pressure profiles retrieved from the IASI are the input for FORLI (Hurtmans et al., 2012). The EUMETSAT data set is not homogenous because the IASI Level 2 product has been processed using different versions in 2008 (v4.2), 2016 (v6.2), 2019 (v6.5), and 2023 (v6.7) (Boynard et al., 2018; Van Damme et al., 2017). Nevertheless, current IASI ozone products are homogeneous and reliable for trend studies (Boynard et al., 2018).

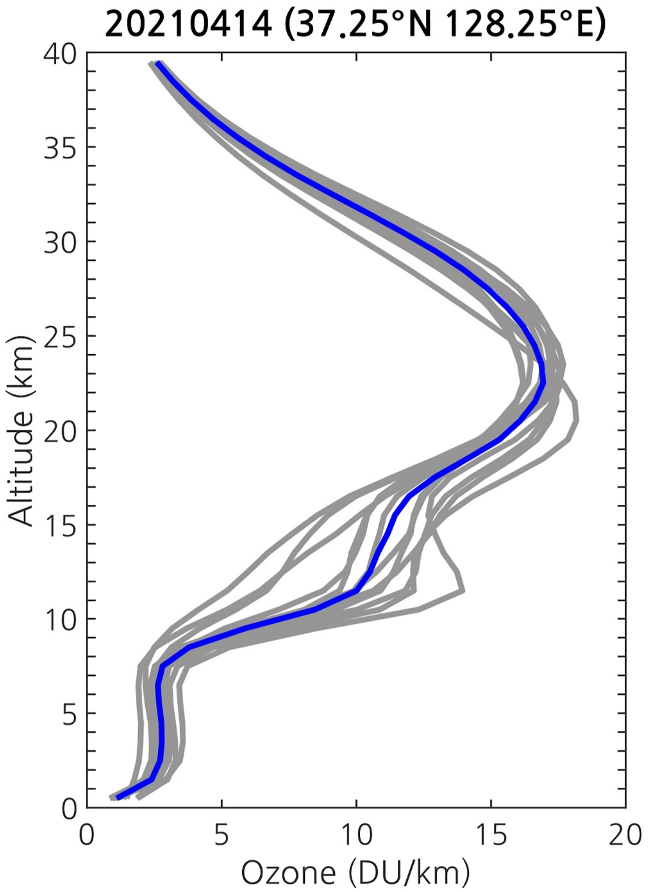

Figure 1. Original ozone profiles from the IASI (gray lines) and a regridded ozone profile (blue line) on 14 April 2021, at 36.25°N, 128.25°E.

The IASI ozone product provides twice-daily global coverage with a 12 km diameter footprint at nadir. Vertical profiles are provided as partial columns in 41 layers, each with a thickness of 1 km, covering altitudes from the surface to 40 km, with an additional layer extending from 40 km to the top of the atmosphere. IASI provides the tropopause altitude based on the World Meteorological Organization (WMO) definition, which is determined using the Lapse Rate Tropopause (Thermal Tropopause). The tropopause altitude is estimated from the IASI L2 atmospheric temperature profile and is given in meters. This study used the IASI ozone products retrieved using FORLI-O3 v20151001 between January 2008 and December 2023. Previous studies have demonstrated the ability of IASI to measure ozone profiles (Boynard et al., 2016, 2018 and references therein). As recommended in Boynard et al. (2018), to ensure data quality, only retrievals associated with a general quality flag (GQF) equal to 1 are used. It is also recommended to exclude data associated with low total degrees of freedom for the signal (DOFS < 2), as this limitation often affects polar region data, such as from Antarctica.

Because of the IASI spatial and temporal non-uniform sampling, the data were interpolated onto a uniform grid to generate global daily maps. We regridded all daytime IASI (IASI-A, IASI-B, and IASI-C) ozone profiles into a 0.5° × 0.5° common grid using the inverse distance weighting (IDW) method (see Figure 1). IDW is a widely used spatial interpolation technique that estimates values at unsampled locations based on the values of nearby sampled points. Interpolated value at a given location is computed as a weighted average of the surrounding data points.

2.2. Ozonesonde Data

An ozonesonde is a balloon-borne instrument that measures the vertical profile of ozone from the surface up to approximately 35 km using an electrochemical concentration cell (ECC) sensor, with an effective vertical resolution of 100–150 m (Tarasick et al., 2021; Thompson et al., 2019). Data collected by an ECC-type ozonesonde has an uncertainty of 5%–10% depending on altitude (Kivi et al., 2007; Smit et al., 2007). Ozonesonde measurements were used to validate the IASI ozone profile in the UTLS layer over East Asia. Data from four ozonesonde stations in East Asia for the period from 2008 to 2023 were downloaded from the World Ozone and Ultraviolet Radiation Data Centre (WOUDC). The stations used were Pohang (36.03°N, 129.38°E), Tsukuba (36.06°N, 140.13°E), Sapporo (43.06°N, 141.33°E), and Naha (26.21°N, 127.69°E), as shown in Figure S1 in Supporting Information S1. These stations launch ozonesondes approximately once a week. The Pohang and Tsukuba stations covered ozonesonde observations from 2008 to 2023, whereas the Sapporo and Naha stations provided data only until 2018.

2.3. Comparison Methodology

To ensure the reliability of the IASI ozone profiles, a comprehensive validation was conducted using ozonesonde measurements from four stations in East Asia. Ozonesonde measures ozone concentration every second, with an inherent response time of approximately 20–30 s. This response time corresponds to a vertical resolution of about 80–150 m (Smit & Kley, 1998; Tarasick et al., 2021). Therefore, ozonesonde profiles were interpolated with 0.1 km intervals to minimize small-scale perturbations and random observation errors (Park et al., 2012). Then, these profiles were compared to IASI ozone profiles, employing a coincidence criterion that covered a 50 km search radius and ±6 hr. A convolution process based on Rodgers (2000) was used to validate satellite ozone profiles, accounting for the differences in vertical resolution. This convolution process is represented by the equation below:

$$x_{\text{smoothed}} = x_{\text{a}} + \text{A}(x_{\text{sonde}} - x_{\text{a}})$$

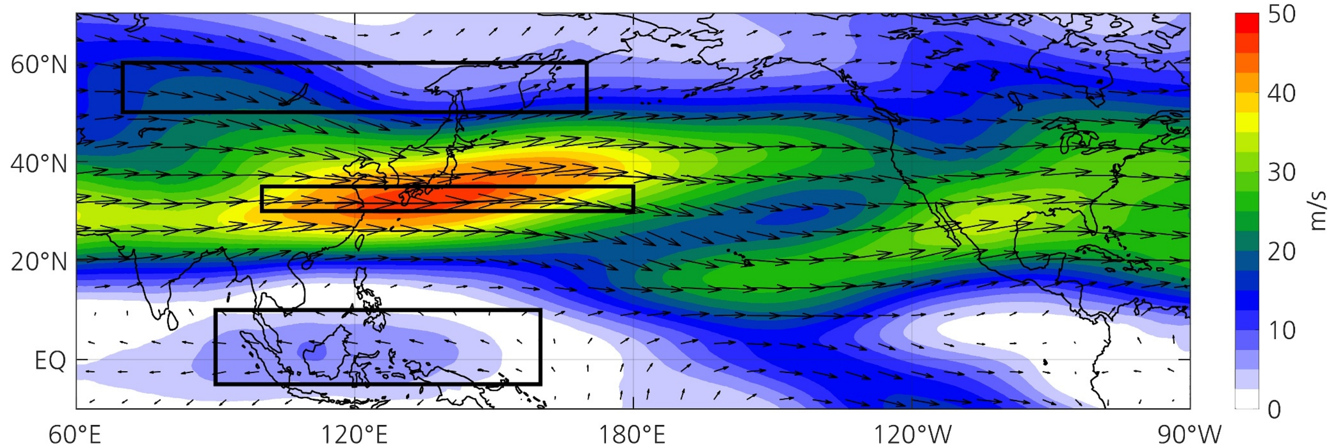

Figure 2. Wind climatology at 200 hPa for the boreal spring (MAM) in MERRA-2. The three boxes represent the EAJSI regions.

where $x_{smoothed}$ is the smoothed ozonesonde profile, x_{sonde} is the ozonesonde profile interpolated on the IASI vertical grid, x_a is the IASI a priori profile, and A is the IASI averaging kernel matrix. An example of the IASI averaging kernel is shown in Figure S2 in Supporting Information S1. If ozonesonde measurements do not cover the entire atmosphere, the profile may be extended using an a priori profile.

IASI exhibits high sensitivity in the UTLS layer (see Figure S2 in Supporting Information S1), corresponding on average to the 8–15 km altitude range (Boynard et al., 2018). Its maximum sensitivity is typically located near the midpoint of the layer, offering approximately one piece of information within this region (Boynard et al., 2018; Wespes et al., 2016). In this study, we define the UTLS partial column for each grid as extending from 4 km below to 2 km above the climatological tropopause of that grid, encompassing the 1 km vertical grid level that includes the tropopause itself. Given a vertical grid resolution of 1 km, this corresponds to a total of seven vertical grid levels encompassing the tropopause level.

2.4. Reanalysis Data

We used other atmospheric variables from reanalysis data sets to evaluate the jet stream mechanisms that influence UTLS ozone. Monthly mean data for horizontal winds, potential vorticity, temperature, and thermal tropopause were provided by the Modern-Era Retrospective analysis for Research and Applications version 2 (MERRA-2) reanalysis (Gelaro et al., 2017). We used monthly mean assimilated data (instM_3d_asm, instM_2d_asm) with a horizontal resolution of 0.5° × 0.625° and 42 pressure levels ranging from 1,000 to 0.01 hPa. All variables were analyzed for the March–April–May (MAM) season from 2008 to 2023 to examine interannual variability. To minimize discrepancies across data sets, all variables were analyzed in their original grid size. To ensure consistency in our analysis, we note that the IASI data set utilizes a z-coordinate system (in meters), whereas the MERRA-2 reanalysis data set employs a pressure coordinate system (in hPa). This fundamental difference in vertical representation poses challenges for direct intercomparison between the two data sets. Therefore, we conducted separate analyses for each data set to account for their respective coordinate frameworks.

2.5. East Asian Jet Stream Index (EAJSI)

The EAJS is strongly linked to atmospheric circulation patterns over East Asia, particularly in the upper levels of the troposphere (Li & Yang, 2010; Yang et al., 2002). To represent the interannual variability in the strength of the jet stream during the boreal spring, we used the EAJSI from Lee et al. (2020). The EAJSI was defined based on the East Asian Winter Monsoon Index (EAWMI) by Li and Yang (2010). The index captures the mean intensity of the cyclonic circulation anomalies to the north of the jet and the anticyclonic anomalies to the south. The wind averaging regions have been adjusted to reflect the climatological mean position of the jet stream during boreal spring, ensuring consistency with its time-mean structure (Lee et al., 2020). The details of the selected regions are shown in Figure 2. The EAJSI was calculated as follows:

10.1029/2024JD043183

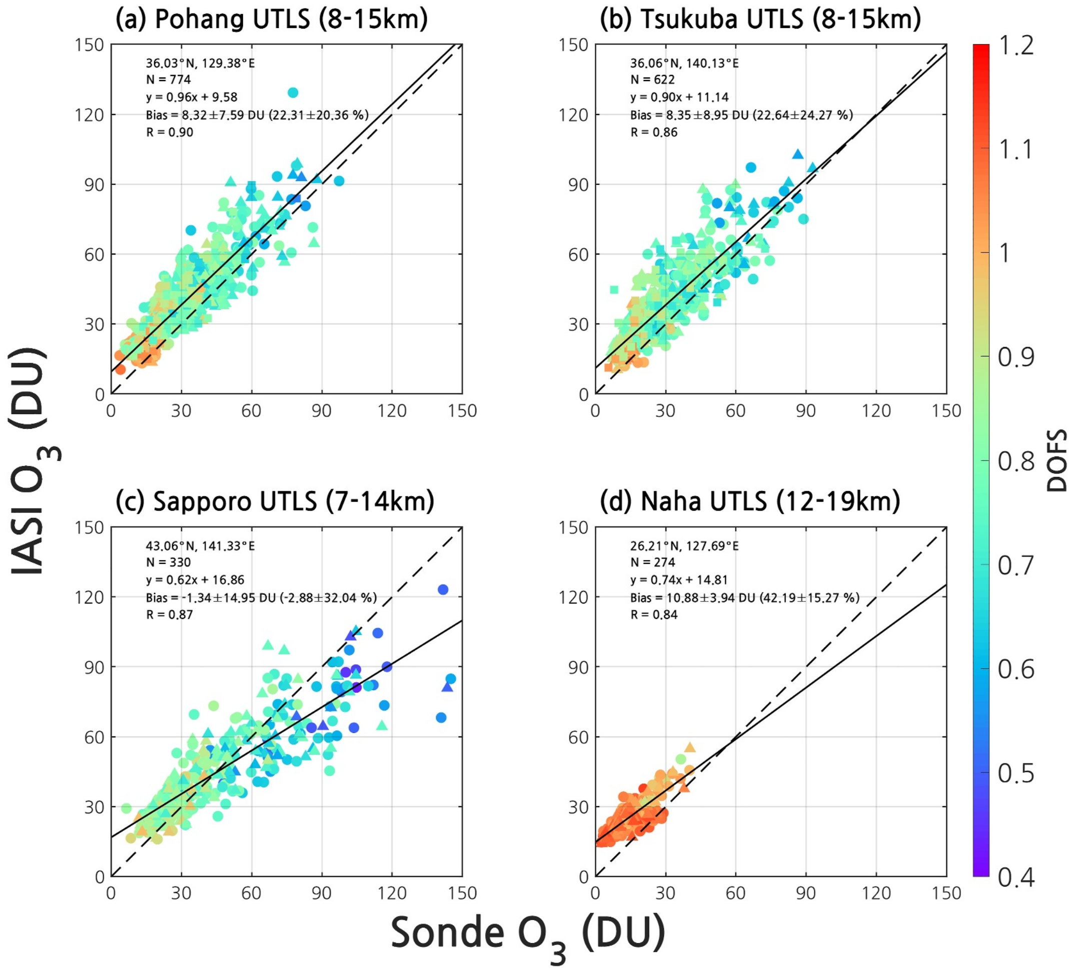

Figure 3. Scatterplots of IASI data against smoothed ozonesonde UTLS O_3 partial columns at (a) Pohang, (b) Tsukuba, (c) Sapporo, and (d) Naha. The circle, triangle, and square symbols represent IASI-A, IASI-B, and IASI-C, respectively. The color of each scatter plot indicates that DOFS values correspond to the UTLS columns.

$$\begin{aligned}\mathrm{EAJSI} = \{&[U_{200}(30°\text{–}35°\mathrm{N}, 100°\text{–}180°\mathrm{E}) – U_{200}(50°\text{–}60°\mathrm{N}, 70°\text{–}170°\mathrm{E})] \\ &+ [U_{200}(30°\text{–}35°\mathrm{N}, 100°\text{–}180°\mathrm{E}) – U_{200}(5°\mathrm{S}\text{–}10°\mathrm{N}, 90°\text{–}160°\mathrm{E})]\}/2.\end{aligned}$$

where U_{200} represents the zonal wind at 200 hPa from the MERRA-2 reanalysis data set, and the monthly mean wind was calculated for the MAM season. The EAJSI was normalized by its standard deviation.

3. Results

3.1. Validation of IASI Results With Ozonesonde Data

Figure 3 shows the validation results of the UTLS partial columns from IASI ozone profiles against the smoothed ozonesonde data for each of the four stations (Pohang, Tsukuba, Sapporo, and Naha), covering the period from 2008 to 2023. The comparison revealed a strong agreement between the IASI and ozonesonde measurements, with correlation coefficients ranging from 0.84 to 0.90 across all stations. The slopes of the linear regression lines ranged from 0.62 to 0.96. The lowest slope was observed at the Sapporo station, likely due to the lower thermal sensitivity in this region, which may affect the accuracy of ozone measurements by IASI. Snow cover and low surface temperatures can reduce the spectral signal-to-noise ratio, resulting in lower DOFS values and limited information content in IASI observations (Boynard et al., 2018). Another possible reason could be the reliance on a single a priori profile (Boynard et al., 2018; Hurtmans et al., 2012), as FORLI utilizes only one, specifically the

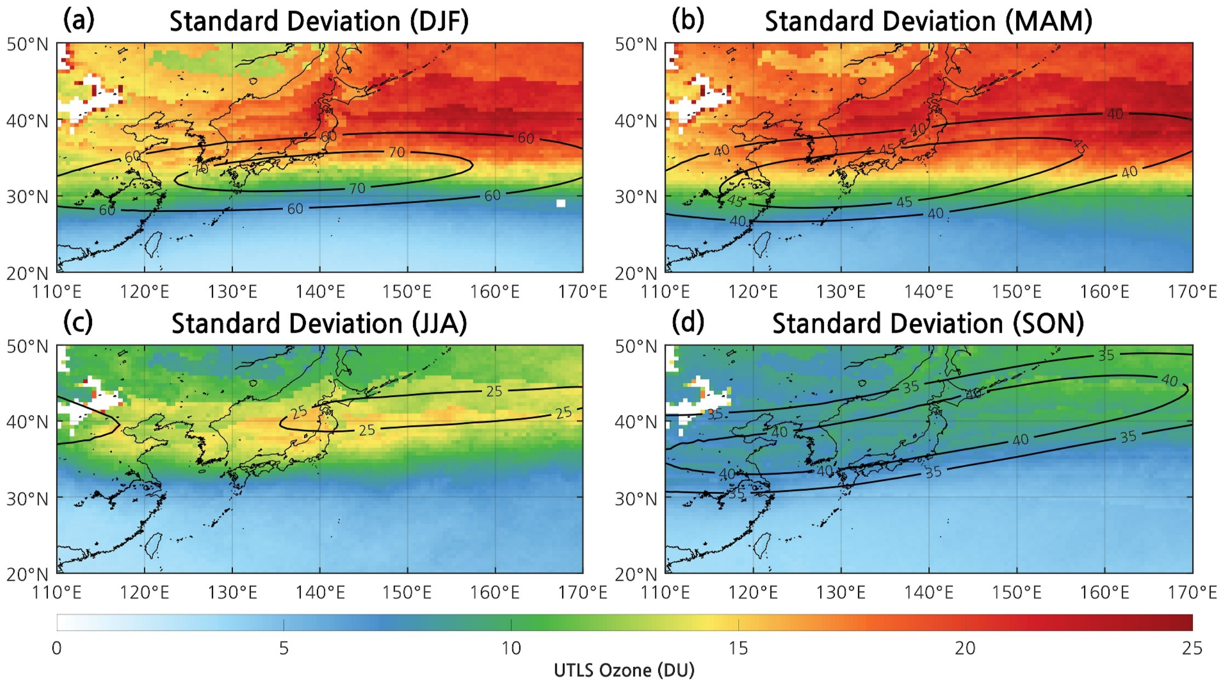

Figure 4. Standard deviation of UTLS ozone (DU) in East Asia for (a) DJF, (b) MAM, (c) JJA, and (d) SON. Contour lines indicate the climatological zonal wind (m/s) at 200 hPa, with values based on the maximum wind speed, to highlight the location of the climatological jet stream.

global mean profile of the McPeters/Labow/Logan climatology (McPeters et al., 2007). The discrepancies in the Sapporo data set are primarily observed when the IASI-derived ozone values exceed 90 DU, suggesting potential retrieval limitations at higher ozone concentrations against a single a priori profile. The reasonable agreement with ozonesonde data, both in terms of correlation coefficients and regression slopes, underscored the capability of IASI to provide reliable ozone profiles. In addition, the DOFS values, which correspond to the number of independent pieces of information that the IASI can provide regarding the ozone profile, varies from 0.6 to 1 with respect to the UTLS columns. The IASI ozone retrieval demonstrates adequate information content within the UTLS layer, enabling it to diagnose the dynamical variability of ozone distribution.

3.2. UTLS Ozone Variability Over East Asia (2008–2023)

After the validation process, we analyzed the seasonal variability of UTLS ozone, as defined in Section 2.3, over East Asia, identifying higher variability in winter and spring, and lower variability in summer and autumn, as shown in Figure 4. These differences highlight the importance of examining seasonal ozone patterns, particularly in springtime, which displayed the most significant variability. The seasonal differences were likely driven by the varying meteorological conditions, including changes in the jet stream and stratosphere-troposphere exchange processes, which are more pronounced during winter and spring (Akritidis et al., 2021; Holton et al., 1995; Stohl et al., 2003; Škerlak et al., 2014). The pronounced variability in these seasons underscored the need for a detailed examination, particularly in springtime (MAM), which had the most significant variability among the seasons analyzed.

To examine the variability of MAM UTLS ozone over East Asia (20°N–50°N, 110°E–170°E) we performed an empirical orthogonal function (EOF) analysis on monthly MAM data from 2008 to 2023. The first three EOF modes and their corresponding principal components (PCs) accounted for 53.8%, 10.8%, and 6.4% of the total variance, respectively. We primarily focused on the first principal component (PC1), which explained more than half of the total variance. Figure 5a shows the correlation between PC1 and UTLS ozone over East Asia, revealing a significant positive correlation, particularly north of 30°N, including Korea, Japan, and parts of China. These regions are heavily influenced by the East Asian jet stream (EAJS), which plays a pivotal role in modulating tropospheric ozone levels during winter and spring, as previously noted by Austin and Midgley (1994). The jet stream's influence was evident in the strong correlation observed between PC1 and the EAJSI, with a correlation

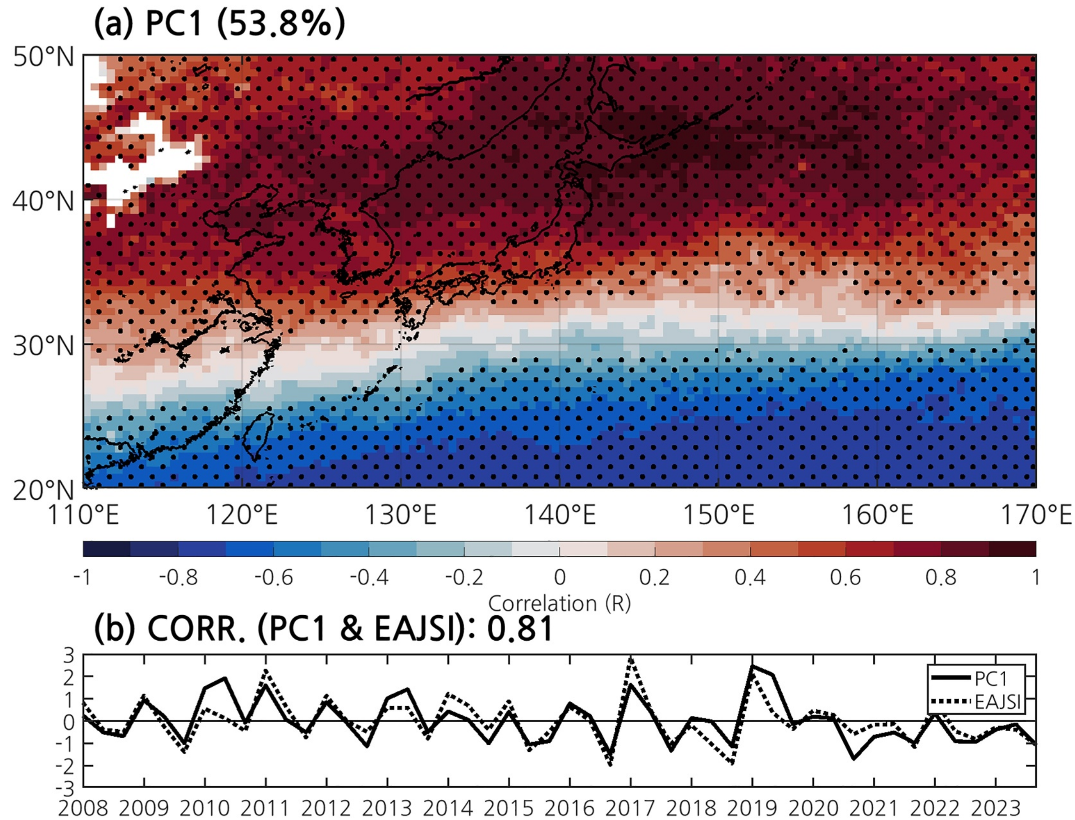

Figure 5. (a) Correlation map of MAM monthly IASI UTLS ozone against PC1. Stippling indicates statistical significance at the 95% confidence level. (b) Time series of PC1 and the EAJSI. The correlation coefficient between PC1 and EAJSI was 0.81.

coefficient of 0.81 (Figure 5b). This finding suggests that variability in UTLS ozone is closely linked to the jet stream, indicating that interannual changes in jet stream strength and position can significantly impact ozone concentrations in the UTLS layer. Further analysis of synoptic dynamics, including an examination of the specific patterns, is essential to fully understand the mechanisms behind the observed correlations. The strong linkage between PC1 and EAJSI underscored the importance of jet stream variability in influencing ozone levels, and therefore PC1 was used in subsequent correlations and regression analyses to explore the dynamics of ozone variability in greater detail.

To cross-check the findings from the EOF analysis and further explore the vertical structure of ozone variability, we conducted a correlation analysis using monthly averaged MAM ozonesonde data and IASI profiles at Pohang and Tsukuba from 2008 to 2023. Sapporo and Naha stations reported data only until 2018 and were therefore excluded from this analysis. Figure 6 shows the vertical distribution of the correlation coefficients between PC1 and ozone profiles determined from both ozonesonde (original) and IASI data. The mean correlation coefficients in the UTLS layer derived from ozonesonde measurements were 0.34 for Tsukuba and 0.30 for Pohang. In comparison, the corresponding correlation coefficients obtained from IASI data were 0.53 for Tsukuba and 0.55 for Pohang. Ozonesonde observations were launched once a week, so the limited number of samples per month may have led to a lower correlation when analyzing monthly mean ozone concentrations. Significant positive correlations were found in the UTLS layer (8–15 km) in both regions, highlighting the meaningful consistency between PC1 from IASI and the observed ozone profiles. These results further supported the notion that the variability captured by PC1 was spatially consistent and extended vertically, influencing the UTLS.

3.3. Relationship Between UTLS Ozone Variability and Large-Scale Circulation

To further investigate the spatial distribution of this variability, Figure 7a presents the linear regression coefficients of UTLS ozone against PC1 across East Asia. The results indicated that positive (negative) PC1 values

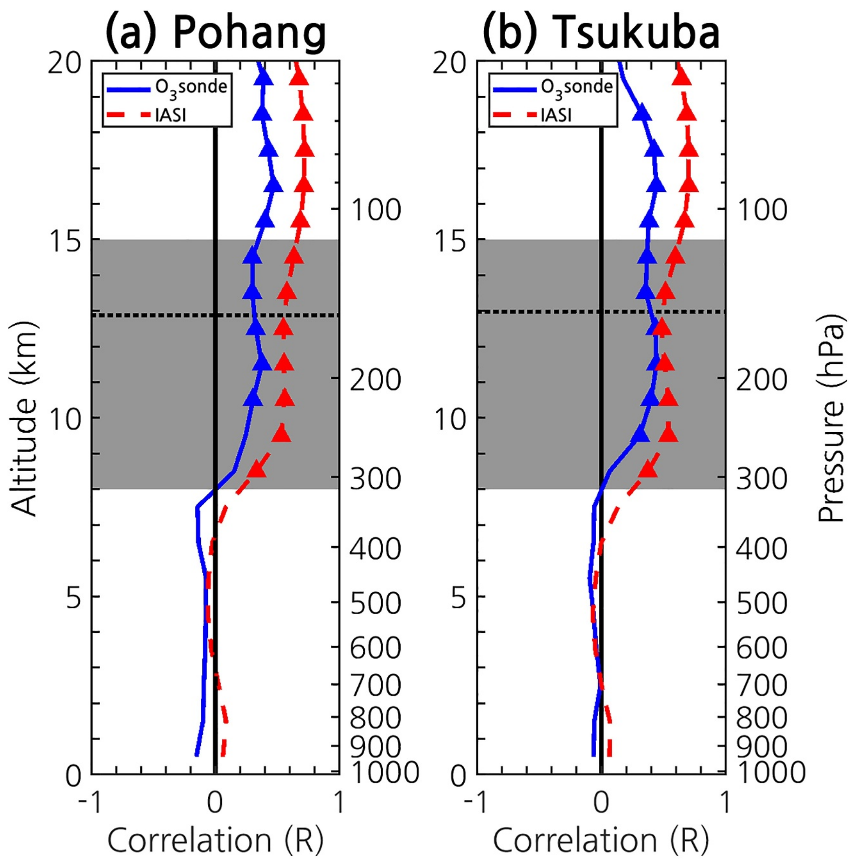

Figure 6. Vertical distribution of the correlation coefficient of the MAM monthly ozone concentration against the PC1 between 2008 and 2023 in (a) Pohang and (b) Tsukuba. The blue solid line represents the ozonesonde observation, whereas the red dashed line represents the IASI observation. Triangle symbols denote statistical significance at the 95% confidence level. The gray region indicates the UTLS (8–15 km) layer. The dotted line indicates the climatological tropopause determined from the IASI data.

were associated with increases (decreases) in UTLS ozone, with values ranging from 5 to 10 DU. The results for the Tibetan Plateau are not shown because the estimation of the tropopause height was not possible with the IASI L2 temperature profile due to the high elevation in the region. To conduct a more detailed assessment of the ozone response to PC1 at different altitudes, we performed a zonal averaging of ozone between 125°E and 145°E. The regression results, shown in Figure 7b, suggest that ozone increased in UTLS over subtropics, with notable ozone increases observed below the climatological tropopause between 35°N and 40°N, particularly over East Asia. Weak negative ozone anomalies were observed between 10°N and 20°N, possibly due to tropical upwelling. These will be further discussed in Section 3.3.2. The positive ozone pattern in UTLS over East Asia may suggest a possible interaction between the stratosphere and troposphere, where ozone-rich air from the stratosphere could be transported downward into the upper troposphere. Although stratospheric intrusions are often linked to tropopause folding events—where isentropic surfaces dip sharply, facilitating the downward transport of stratospheric air—this study does not explicitly quantify such processes.

3.3.1. Jet Stream Intensification and Its Role in UTLS Ozone Variability

The correlation of PC1 with atmospheric dynamics over East Asia during the boreal spring (MAM) is shown in Figure 8. There was a significant strengthening of the EAJS with positive wind anomalies in response to PC1 (Figure 8a). The enhanced jet stream was consistent with the findings from the EAJSI analysis, which exhibited a strong correlation with PC1. This response was consistent with the intensity of the EAJSI results reported by Manney and Hegglin (2018) and Chan et al. (2020), although the region defined for the EAJSI in our study was more extensive. The strengthening of the EAJS was most pronounced between 30°N and 40°N, with an extension from central to East Asia. Moreover, two zonally extended negative anomalies were observed on the meridional

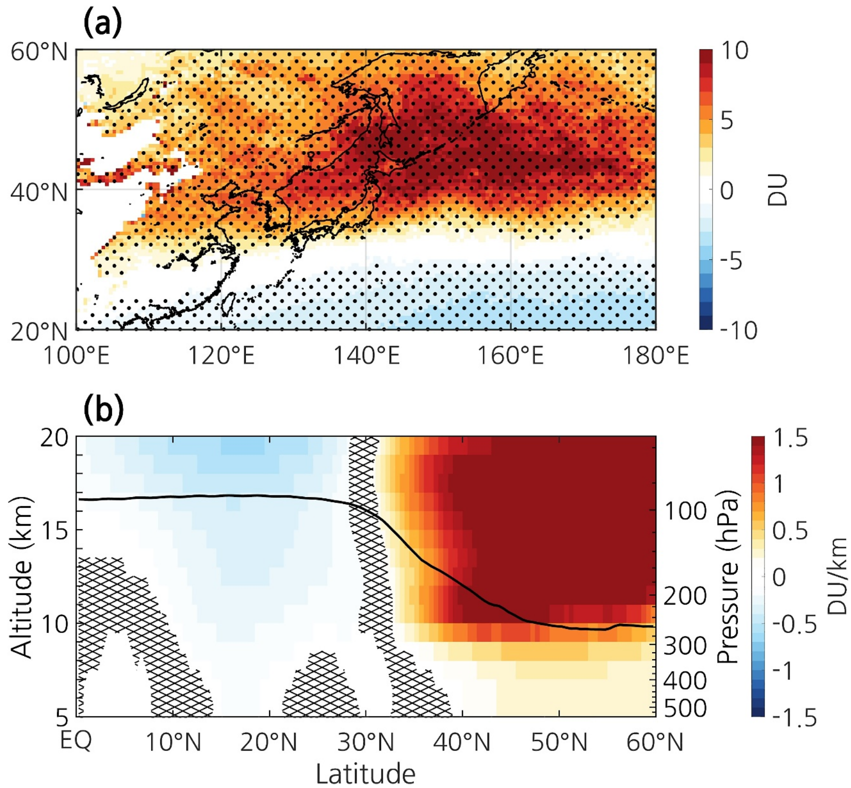

Figure 7. (a) Regression patterns for monthly IASI UTLS ozone (DU) against PC1 over East Asia. Stippling indicates statistical significance at the 95% confidence level. (b) Regression patterns for the zonal-averaged (125°E–145°E) monthly IASI ozone concentration (shaded, unit: DU/km) against the PC1. Crosshatched areas indicate statistical nonsignificance at the 95% confidence level. The thick black lines represent the climatological thermal tropopause estimated from the IASI temperature profile.

sides of the positive wind anomaly, indicating that a meridional sharpening of the jet occurred with an intensified jet (Chan et al., 2020; Yang et al., 2002).

The poleward transient eddy heat flux serves as a proxy for the intensity of baroclinic waves because it reflects the meridional transport of heat and moisture, which indicates baroclinic instability (Chang et al., 2002). Figure 8b shows the regression pattern of storm track activity, calculated using the poleward heat flux at 850 hPa. The positive anomalies in storm track activity between 20°N and 40°N suggesting enhanced baroclinic instability. Tropopause folding is linked to baroclinic developments associated with very strong jet streams (Austin & Midgley, 1994; Holton et al., 1995; Shapiro, 1980). As baroclinic wave activity develops near the tropopause, it can influence the breaking of Rossby waves and induce strong subsidence (Lamarque & Hess, 1994; Holton et al., 1995, and references therein). We found an intensification of baroclinic wave development associated with the intensification of the EAJS in the mid-latitudes, particularly over the North Pacific and East Asia, during periods of positive PC1.

Figure 8c shows the regression pattern of potential vorticity at 200 hPa on PC1, which can be used as a stratospheric tracer, with positive potential vorticity anomalies indicating areas of enhanced subsidence. The observed significant positive potential vorticity anomalies observed at 200 hPa over East Asia, particularly between 30°N and 50°N, are indicative of enhanced stratosphere-troposphere exchange processes. The alignment of these potential vorticity anomalies with increases in ozone concentration, as shown in Figure 7a, reinforces the concept of stratospheric intrusions. The strengthening of the EAJS appears to play a pivotal role in facilitating these stratospheric intrusions. A stronger jet stream can enhance the baroclinic wave activity, leading to more frequent and intense tropopause folding events. These events create pathways for stratospheric air to enter the troposphere, thus contributing to the observed positive potential vorticity anomalies. The enhanced subsidence associated with

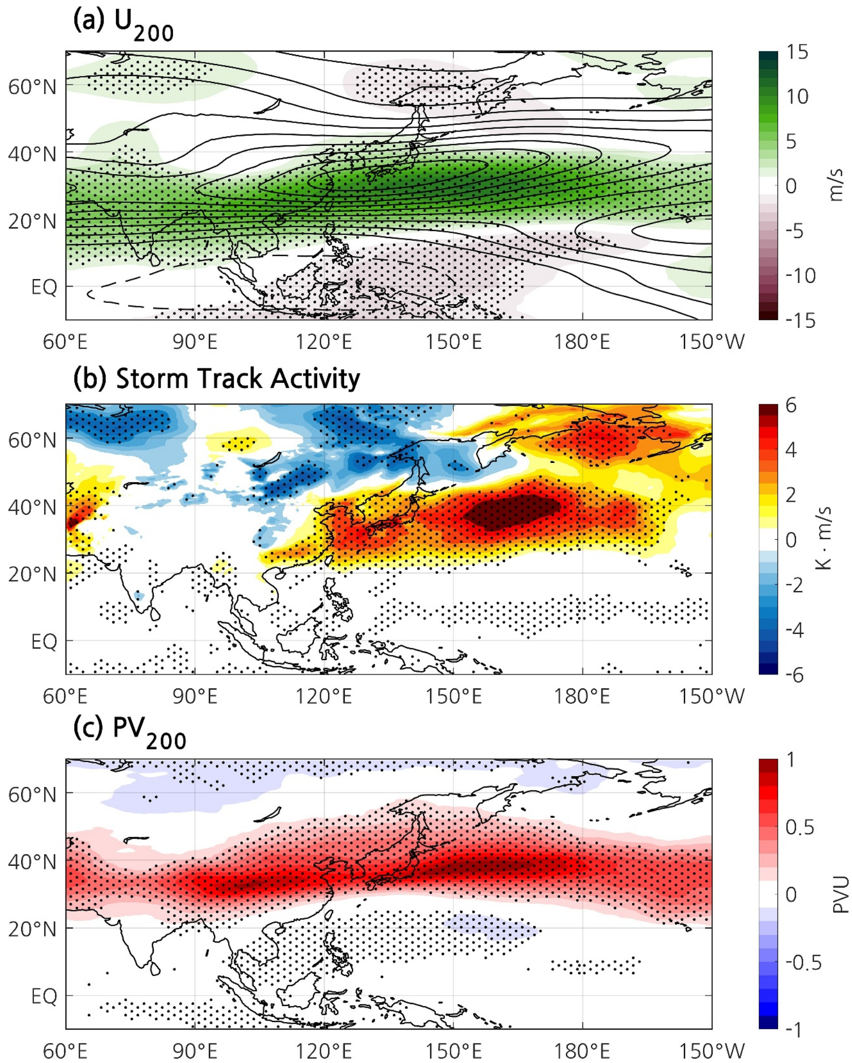

Figure 8. Regression patterns for MERRA-2 (a) zonal wind at 200 hPa (shaded, unit: m/s), (b) storm track activity at 850 hPa (shaded, unit: K m/s), and (c) potential vorticity at 200 hPa (shaded, unit: PVU) against PC1. The contour lines in (a) are the climatological zonal wind (interval: 10 m/s) at 200 hPa for the boreal spring (MAM). Stippling indicates statistical significance at the 95% confidence level.

the potential vorticity anomalies typically leads to the downward transport of ozone-rich air, indicating stratospheric intrusion and resulting in the observed increase in UTLS ozone levels.

To further assess the zonal-vertical structure, a regression analysis was conducted on the zonally averaged zonal wind and potential vorticity between 125°E and 145°E. Figure 9 presents the regression patterns of these variables against PC1, providing additional insights into the vertical and latitudinal dependencies of the atmospheric circulation anomalies associated with ozone variability. There were significant wind anomalies near the jet stream core, with a pronounced increase in zonal wind speeds centered around 30°N, particularly between 200 and 100 hPa. This corresponds to the region and pressure levels where the EAJS is typically most intense. The regression results indicate that positive PC1 values were associated with a strengthening and slight equatorward shift of the jet stream, reinforcing the findings from the horizontal wind analysis. We also found a significant positive potential vorticity anomaly between 30°N and 50°N, particularly below the tropopause. This increase in potential vorticity near the tropopause is a key indicator of the stratospheric air influx, which is typically rich in ozone. This result supports the interpretation that the increase in the ozone concentration observed in Figure 7b was the result of stratosphere-troposphere exchanges.

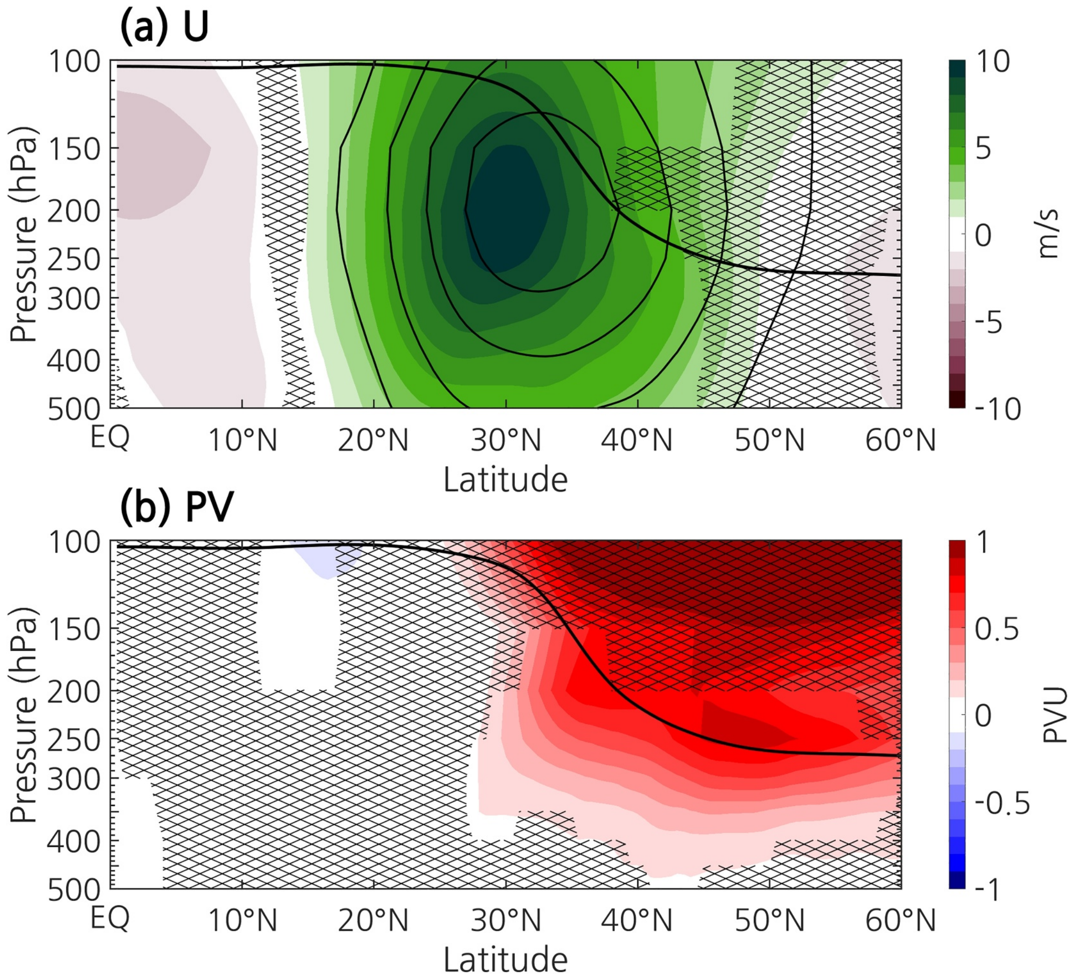

Figure 9. Regression patterns for zonal-averaged (125°E–145°E) (a) zonal wind (shaded, unit: m/s), and (b) potential vorticity (shaded, unit: PVU) against PC1. The contour lines shown in (a) are the climatological zonal wind (interval: 10 m/s) for the boreal spring (MAM). Crosshatched areas indicate statistical nonsignificance at the 95% confidence level. The thick black lines represent the climatological thermal tropopause in MERRA-2.

In summary, our results prove that the intensification of the EAJS is linked with baroclinic wave development (as measured using the poleward heat flux at 850 hPa) and is also associated with stratospheric intrusion which modulates ozone levels during the boreal spring. This suggests that variation in the jet stream's intensity is closely linked to the observed ozone variability in the UTLS layer. The strengthening of the jet stream likely enhances the transport of ozone-rich air from the stratosphere into the upper troposphere, contributing to higher ozone concentrations in East Asia. Our findings contrast with the situation in the western United States, where Lin et al. (2015) found that high-ozone events were influenced by stratospheric intrusions associated with meandering polar jets. However, our findings align with those of Hwang et al. (2007), who found that the secondary ozone peak in Pohang was closely linked to strong zonal wind speeds near the jet core, as observed in ozonesonde data. East Asia experiences frequent stratospheric intrusions driven by an intensified jet stream, in contrast to the pattern observed in the western United States. The observed enhancement of UTLS ozone levels over East Asia during the positive phase of PC1 may indicate a role for stratospheric intrusions in UTLS ozone variability; however, further investigation is required to confirm and quantify this mechanism.

3.3.2. Main Drivers Causing Jet Stream Variability

The Hadley circulation and jets are both related to baroclinic instability in tropical and subtropical regions, and the time-averaged subtropical jet appears at the same location as the boundary of the Hadley circulation (Held & Hou, 1980). Moreover, when convection over the western tropical Pacific is strong, the EAJS tends to strengthen

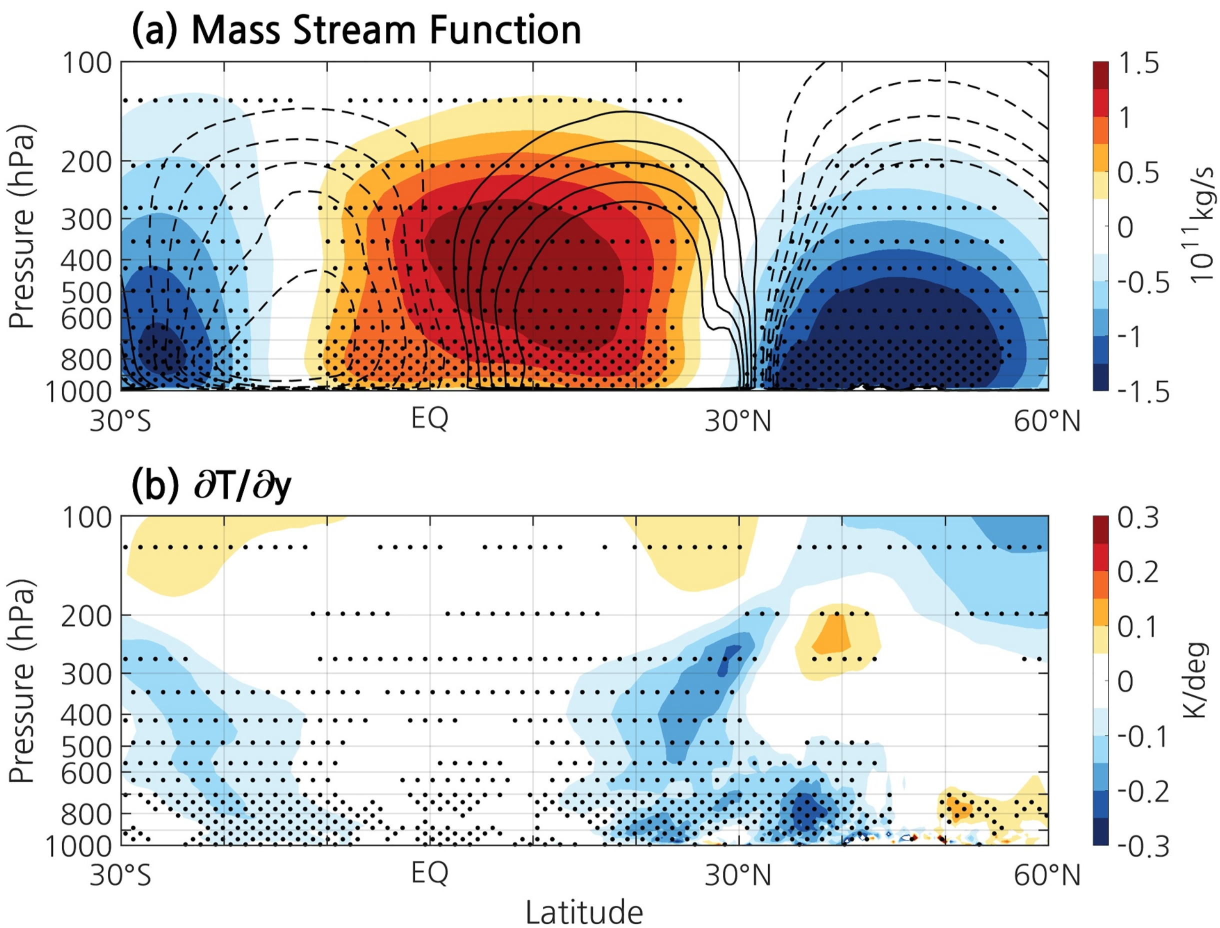

Figure 10. Regression patterns for zonal-averaged (80°E–120°E) (a) mass stream function (shaded, unit: 10^{11} kg/s) and (b) meridional temperature gradient (shaded, unit: K/deg) against PC1. Stippling denotes statistical significance at the 95% confidence level. The solid and dashed contours indicate the climatological positive mass stream function (interval: 4×10^{10} kg/s) and negative mass stream function (interval: 4×10^{10} kg/s) for the boreal spring (MAM), respectively.

due to its influence on the local Hadley circulation (Chan et al., 2020; Park & An, 2014). The intensification of the jet is initiated by angular momentum from convection over the Bay of Bengal-South China Sea and the Pacific Warm Pool in the upstream region and is maintained by feedback with the Pacific Subtropical oceanfront through eddy interactions in the downstream region (Chan et al., 2020). To further examine the mechanisms contributing to EAJS variability, we analyzed the Hadley circulation and meridional temperature gradient. Figure 10a shows the regression pattern of the mass stream function averaged over the upstream region (80°E–120°E) against PC1, revealing enhanced upward motion over the tropics and strengthened local Hadley Cells in the Northern Hemisphere with a positive PC1. These findings support the idea that convectively driven local Hadley cells are key drivers of the EAJS intensification over the upstream region, even during springtime, which agrees with previous studies (Chan et al., 2020; Manney & Hegglin, 2018; Park & An, 2014). Moreover, intensified tropical upwelling can lead to a reduction in ozone over the tropics, as shown in Figure 7b (Butchart, 2014). As most of the shallow branch is likely located below 70 hPa, this may be attributed to the influence of the shallow branch of the Brewer-Dobson circulation in the tropics (Butchart, 2014).

The corresponding anomalous meridional temperature gradient is shown in Figure 10b, where the negative anomalies are located around 20°N–40°N. Such a gradient is associated with the EAJS strengthening seen in Figure 8a and is consistent with the thermal wind relationship. The horizontal meridional temperature gradient in the lower troposphere, as well as the average for the mid-to-lower troposphere (Figure S2 in Supporting Information S1), exhibited negative anomalies around 20°N–40°N. These anomalies aligned with storm-track activity, indicating enhanced baroclinic instability. Therefore, local Hadley cells and the meridional temperature gradient could contribute to an intensification of the EAJS.

Jeong et al. (2023) reported a positive ozone anomaly between 300 and 200 hPa and an intensification of the jet streams over South Korea in springtime after the La Niña peak, although the underlying mechanisms remain unknown. In the case of the El Niño, the EAJS tends to shift eastward, intensifying over the North Pacific while weakening over East Asia (Li & Yang, 2010; Manney et al., 2021; Trenberth et al., 1998; Yang et al., 2002). Conversely, during La Niña periods, when convection over the western tropical Pacific is strong, the EAJS tends to strengthen due to its influence on the local Hadley circulation (Chan et al., 2020; Park & An, 2014). Our results indicate that the intensification of the jet stream is associated with increased UTLS ozone. This suggests a partial linkage of the observed increase in the tropospheric column ozone over East Asia following the La Niña peak (Jeong et al., 2023; Wie et al., 2021), which is likely driven by the intensification of the East Asian jet, resulting from enhanced convection in the western Pacific and the strengthening of the local Hadley cells.

4. Summary and Discussion

We examined the springtime variability of UTLS ozone over East Asia in association with the jet stream using IASI satellite data, ozonesonde observations, and MERRA-2 reanalysis data. We utilized ozone profile data from the IASI on the Metop-A, Metop-B, and Metop-C satellites, validated against ozonesonde measurements from four East Asian stations. The IASI ozone profiles, retrieved using the FORLI-O3 algorithm, were reliable, with reasonable correlations with ozonesonde data, confirming their suitability for studying UTLS ozone dynamics. An EOF analysis identified that the PC1 explained more than half of the total variance in UTLS ozone during springtime, with strong positive correlations observed over regions heavily influenced by the East Asian jet, including Korea, Japan, and parts of China. The relationship between PC1 and the EAJSI highlighted the pivotal role of the jet stream in modulating ozone levels in the UTLS layer over East Asia. Strengthening of the East Asian jet is associated with increased ozone concentrations over East Asia, and is linked to baroclinic wave activity and enhanced stratospheric intrusion. These findings were supported by a regression analysis, which demonstrated that positive PC1 phases were associated with increased zonal wind and potential vorticity anomalies. This was indicative of the downward transport of ozone-rich air from the stratosphere. The results highlighted the importance of the jet stream as a key driver of UTLS ozone variability over East Asia. Variation in jet stream strength and position significantly impacts the vertical and spatial distribution of ozone, contributing to observed seasonal and interannual changes. Moreover, jet stream variability is closely linked to the local Hadley cell and the meridional temperature gradient, suggesting that further studies are required to determine the impact of broader climate variability on UTLS ozone concentrations over East Asia.

This study provides valuable insights into the mechanisms driving ozone variability in the UTLS over East Asia, highlighting the critical role of jet stream variation in influencing ozone distribution. The strong correlations identified across multiple data sets and methodologies provide compelling evidence that jet stream dynamics significantly modulate ozone levels, which has important implications for regional climate and air quality. In addition, this study demonstrated the value of the vertical profile of atmospheric composition from infrared sounders, such as the IASI, for advancing our understanding of UTLS ozone dynamics. Future research should continue to leverage these observational tools to explore the impacts of other large-scale climate modes, such as the ENSO and Pacific Decadal Oscillation (PDO), on UTLS ozone variability.

Acknowledgments
This work was supported by a National Research Foundation of Korea (NRF) grant funded by the Korean government under the Ministry of Science and Information & Communications Technology (MSIT) (RS-2023–00219830 and NRF-2023R1A2C1004083). The IASI mission is a joint mission of Eumetsat and the Centre National d'Etudes Spatiales (CNES, France). The IASI L1 and L2 data are distributed in near real time by Eumetsat through the Eumetcast system distribution. The authors acknowledge the AERIS data infrastructure (https://www.aeris-data.fr) for providing access to the IASI Level 1 radiance and to the IASI Level 2 data.

Data Availability Statement

IASI data are available from the AERIS data portal for each Metop platform: Metop-A (https://iasi.aeris-data.fr/ozos_iasi_a_arch/), Metop-B (https://iasi.aeris-data.fr/ozos_iasi_b_arch/), and Metop-C (https://iasi.aeris-data.fr/ozos_iasi_c_arch/). Ozonesonde observations are archived at https://woudc.org/home.php. MERRA-2 data set was obtained from https://doi.org/10.5067/2E096JV59PK7 and https://doi.org/10.5067/5ESKGQTZG7FO.

References

Akritidis, D., Pozzer, A., Flemming, J., Inness, A., & Zanis, P. (2021). A global climatology of tropopause folds in CAMS and MERRA-2 reanalyses. *Journal of Geophysical Research: Atmospheres*, *126*(8), e2020JD034115. https://doi.org/10.1029/2020JD034115

Austin, J. F., & Midgley, R. P. (1994). The climatology of the jet stream and stratospheric intrusions of ozone over Japan. *Atmospheric Environment*, *28*(1), 39–52. https://doi.org/10.1016/1352-2310(94)90021-3

Boynard, A., Hurtmans, D., Garane, K., Goutail, F., Hadji-Lazaro, J., Koukouli, M. E., et al. (2018). Validation of the IASI FORLI/EUMETSAT ozone products using satellite (GOME-2), ground-based (Brewer–Dobson, SAOZ, FTIR) and ozonesonde measurements. *Atmospheric Measurement Techniques*, *11*(9), 5125–5152. https://doi.org/10.5194/amt-11-5125-2018

Boynard, A., Hurtmans, D., Koukouli, M. E., Goutail, F., Bureau, J., Safieddine, S., et al. (2016). Seven years of IASI ozone retrievals from FORLI: Validation with independent total column and vertical profile measurements. *Atmospheric Measurement Techniques*, *9*(9), 4327–4353. https://doi.org/10.5194/amt-9-4327-2016

Butchart, N. (2014). The Brewer-Dobson circulation. *Reviews of Geophysics*, *52*(2), 157–184. https://doi.org/10.1002/2013RG000448

Chan, D., Zhang, Y., Wu, Q., & Dai, X. (2020). Quantifying the dynamics of the interannual variabilities of the wintertime East Asian Jet Core. *Climate Dynamics*, *54*(3), 2447–2463. https://doi.org/10.1007/s00382-020-05127-3

Chang, E. K. M., Lee, S., & Swanson, K. L. (2002). Storm track dynamics. *Journal of Climate*, *15*(16), 2163–2183. https://doi.org/10.1175/1520-0442(2002)015<02163:STD>2.0.CO;2

Clerbaux, C., Boynard, A., Clarisse, L., George, M., Hadji-Lazaro, J., Herbin, H., et al. (2009). Monitoring of atmospheric composition using the thermal infrared IASI/Metop sounder. *Atmospheric Chemistry and Physics*, *9*(16), 6041–6054. https://doi.org/10.5194/acp-9-6041-2009

Clerbaux, C., Hadji-Lazaro, J., Turquety, S., George, M., Boynard, A., Pommier, M., et al. (2015). Tracking pollutants from space: Eight years of IASI satellite observation. *Comptes Rendus Geoscience*, *347*(3), 134–144. https://doi.org/10.1016/j.crte.2015.06.001

Colombi, N. K., Jacob, D. J., Yang, L. H., Zhai, S., Shah, V., Grange, S. K., et al. (2023). Why is ozone in South Korea and the Seoul metropolitan area so high and increasing? *Atmospheric Chemistry and Physics*, *23*(7), 4031–4044. https://doi.org/10.5194/acp-23-4031-2023

Gelaro, R., McCarty, W., Suárez, M. J., Todling, R., Molod, A., Takacs, L., et al. (2017). The modern-era retrospective analysis for research and applications, version 2 (MERRA-2). *Journal of Climate*, *30*(14), 5419–5454. https://doi.org/10.1175/JCLI-D-16-0758.1

Gettelman, A., Hoor, P., Pan, L. L., Randel, W. J., Hegglin, M. I., & Birner, T. (2011). The extratropical upper troposphere and lower stratosphere. *Reviews of Geophysics*, *49*(3), RG3003. https://doi.org/10.1029/2011RG000355

Held, I. M., & Hou, A. Y. (1980). Nonlinear axially symmetric circulations in a nearly inviscid atmosphere. *Journal of the Atmospheric Sciences*, *37*(3), 515–533. https://doi.org/10.1175/1520-0469(1980)037<0515:NASCIA>2.0.CO;2

Holton, J. R., Haynes, P. H., McIntyre, M. E., Douglass, A. R., Rood, R. B., & Pfister, L. (1995). Stratosphere-troposphere exchange. *Reviews of Geophysics*, *33*(4), 403–439. https://doi.org/10.1029/95RG02097

Hurtmans, D., Coheur, P. F., Wespes, C., Clarisse, L., Scharf, O., Clerbaux, C., et al. (2012). FORLI radiative transfer and retrieval code for IASI. *Journal of Quantitative Spectroscopy and Radiative Transfer*, *113*(11), 1391–1408. https://doi.org/10.1016/j.jqsrt.2012.02.036

Hwang, S.-H., Kim, J., & Cho, G.-R. (2007). Observation of secondary ozone peaks near the tropopause over the Korean peninsula associated with stratosphere-troposphere exchange. *Journal of Geophysical Research*, *112*(D16), D16305. https://doi.org/10.1029/2006JD007978

Jeong, Y., Kim, S.-W., Kim, J., Shin, D., Kim, J., Park, J.-H., & An, S.-I. (2023). Influence of ENSO on tropospheric ozone variability in East Asia. *Journal of Geophysical Research: Atmospheres*, *128*(16), e2023JD038604. https://doi.org/10.1029/2023JD038604

Jeong, Y.-C., Yeh, S.-W., Lee, S., Park, R. J., & Son, S.-W. (2021). Impact of the stratospheric ozone on the Northern Hemisphere surface climate during boreal winter. *Journal of Geophysical Research: Atmospheres*, *126*(17), e2021JD034958. https://doi.org/10.1029/2021JD034958

Kang, S. M., Polvani, L. M., Fyfe, J. C., & Sigmond, M. (2011). Impact of polar ozone depletion on subtropical precipitation. *Science*, *332*(6032), 951–954. https://doi.org/10.1126/science.1202131

Kivi, R., Kyrö, E., Turunen, T., Harris, N. R. P., von der Gathen, P., Rex, M., et al. (2007). Ozonesonde observations in the Arctic during 1989–2003: Ozone variability and trends in the lower stratosphere and free troposphere. *Journal of Geophysical Research*, *112*(D8), D08306. https://doi.org/10.1029/2006JD007271

Lamarque, J.-F., & Hess, P. G. (1994). Cross-tropopause mass exchange and potential vorticity budget in a simulated tropopause folding. *Journal of the Atmospheric Sciences*, *51*(15), 2246–2269. https://doi.org/10.1175/1520-0469(1994)051<2246:CTMEAP>2.0.CO;2

Lee, H.-J., Chang, L.-S., Jaffe, D. A., Bak, J., Liu, X., Abad, G. G., et al. (2021). Ozone continues to increase in east asia despite decreasing NO_2: Causes and abatements. *Remote Sensing*, *13*(11), 2177. https://doi.org/10.3390/rs13112177

Lee, S., Lee, M.-I., Song, C.-K., Kim, K.-M., & da Silva, A. M. (2020). Interannual variation of the East Asia Jet Stream and its impact on the horizontal distribution of aerosol in boreal spring. *Atmospheric Environment*, *223*, 117296. https://doi.org/10.1016/j.atmosenv.2020.117296

Lee, T., Go, S., Lee, Y. G., Park, S. S., Park, J., & Koo, J.-H. (2022). Temporal variability of surface air pollutants in megacities of South Korea. *Frontiers in Environmental Science*, *10*. https://doi.org/10.3389/fenvs.2022.915531

Li, Y., & Yang, S. (2010). A dynamical index for the East Asian winter monsoon. *Journal of Climate*, *23*(15), 4255–4262. https://doi.org/10.1175/2010JCLI3375.1

Lin, M., Fiore, A. M., Horowitz, L. W., Langford, A. O., Oltmans, S. J., Tarasick, D., & Rieder, H. E. (2015). Climate variability modulates western US ozone air quality in spring via deep stratospheric intrusions. *Nature Communications*, *6*(1), 7105. https://doi.org/10.1038/ncomms8105

Manabe, S., & Möller, F. (1961). On the radiative equilibrium and heat balance of the atmosphere. *Monthly Weather Review*, *89*(12), 503–532. https://doi.org/10.1175/1520-0493(1961)089<0503:OTREAH>2.0.CO;2

Manney, G. L., & Hegglin, M. I. (2018). Seasonal and regional variations of long-term changes in upper-tropospheric jets from reanalyses. *Journal of Climate*, *31*(1), 423–448. https://doi.org/10.1175/JCLI-D-17-0303.1

Manney, G. L., Hegglin, M. I., & Lawrence, Z. D. (2021). Seasonal and regional signatures of ENSO in upper tropospheric jet characteristics from reanalyses. *Journal of Climate*, *34*(22), 9181–9200. https://doi.org/10.1175/JCLI-D-20-0947.1

McPeters, R. D., Labow, G. J., & Logan, J. A. (2007). Ozone climatological profiles for satellite retrieval algorithms. *Journal of Geophysical Research*, *112*(D5), D05308. https://doi.org/10.1029/2005JD006823

Nowack, P. J., Luke Abraham, N., Maycock, A. C., Braesicke, P., Gregory, J. M., Joshi, M. M., et al. (2015). A large ozone-circulation feedback and its implications for global warming assessments. *Nature Climate Change*, *5*(1), 41–45. https://doi.org/10.1038/nclimate2451

Pan, L. L., Atlas, E. L., Honomichl, S. B., Smith, W. P., Kinnison, D. E., Solomon, S., et al. (2024). East Asian summer monsoon delivers large abundances of very short-lived organic chlorine substances to the lower stratosphere. *Proceedings of the National Academy of Sciences*, *121*(12), e2318716121. https://doi.org/10.1073/pnas.2318716121

Park, J.-H., & An, S.-I. (2014). The impact of tropical western Pacific convection on the North Pacific atmospheric circulation during the boreal winter. *Climate Dynamics*, *43*(7), 2227–2238. https://doi.org/10.1007/s00382-013-2047-7

Park, S. S., Kim, J., Cho, H. K., Lee, H., Lee, Y., & Miyagawa, K. (2012). Sudden increase in the total ozone density due to secondary ozone peaks and its effect on total ozone trends over Korea. *Atmospheric Environment*, *47*, 226–235. https://doi.org/10.1016/j.atmosenv.2011.11.011

Rodgers, C. D. (2000). *Inverse methods for atmospheric sounding: Theory and practice*. World Scientific. Retrieved from https://books.google.co.kr/books?id=p3b3ngEACAAJ

Shapiro, M. A. (1980). Turbulent mixing within tropopause folds as a mechanism for the exchange of chemical constituents between the stratosphere and troposphere. *Journal of the Atmospheric Sciences*, *37*(5), 994–1004. https://doi.org/10.1175/1520-0469(1980)037<0994:TMWTFA>2.0.CO;2

Škerlak, B., Sprenger, M., & Wernli, H. (2014). A global climatology of stratosphere–troposphere exchange using the ERA-Interim data set from 1979 to 2011. *Atmospheric Chemistry and Physics*, *14*(2), 913–937. https://doi.org/10.5194/acp-14-913-2014

Smit, H. G. J., & Kley, D. (1998). *JOSIE: The 1996 WMO International intercomparison of ozonesondes under quasi flight conditions in the environmental simulation chamber at Jülich*. WMO Global Atmosphere Watch Report No.130, WMO TD No. 926. World Meteorological Organization.

Smit, H. G. J., Straeter, W., Johnson, B. J., Oltmans, S. J., Davies, J., Tarasick, D. W., et al. (2007). Assessment of the performance of ECC-ozonesondes under quasi-flight conditions in the environmental simulation chamber: Insights from the Juelich Ozone Sonde Intercomparison Experiment (JOSIE). *Journal of Geophysical Research*, *112*(D19), D19306. https://doi.org/10.1029/2006JD007308

Son, S.-W., Tandon, N. F., Polvani, L. M., & Waugh, D. W. (2009). Ozone hole and Southern Hemisphere climate change. *Geophysical Research Letters*, *36*(15), L15705. https://doi.org/10.1029/2009GL038671

Stohl, A., Bonasoni, P., Cristofanelli, P., Collins, W., Feichter, J., Frank, A., et al. (2003). Stratosphere-troposphere exchange: A review, and what we have learned from STACCATO. *Journal of Geophysical Research*, *108*(D12), 8516. https://doi.org/10.1029/2002JD002490

Tarasick, D. W., Smit, H. G. J., Thompson, A. M., Morris, G. A., Witte, J. C., Davies, J., et al. (2021). Improving ECC ozonesonde data quality: Assessment of current methods and outstanding issues. *Earth and Space Science*, *8*(3), e2019EA000914. https://doi.org/10.1029/2019EA000914

Thompson, A. M., Smit, H. G. J., Witte, J. C., Stauffer, R. M., Johnson, B. J., Morris, G., et al. (2019). Ozonesonde quality assurance: The JOSIE–SHADOZ (2017) experience. *Bulletin of the American Meteorological Society*, *100*(1), 155–171. https://doi.org/10.1175/BAMS-D-17-0311.1

Trenberth, K. E., Branstator, G. W., Karoly, D., Kumar, A., Lau, N.-C., & Ropelewski, C. (1998). Progress during TOGA in understanding and modeling global teleconnections associated with tropical sea surface temperatures. *Journal of Geophysical Research*, *103*(C7), 14291–14324. https://doi.org/10.1029/97JC01444

Van Damme, M., Whitburn, S., Clarisse, L., Clerbaux, C., Hurtmans, D., & Coheur, P. F. (2017). Version 2 of the IASI NH3 neural network retrieval algorithm: Near-real-time and reanalysed datasets. *Atmospheric Measurement Techniques*, *10*(12), 4905–4914. https://doi.org/10.5194/amt-10-4905-2017

Wespes, C., Hurtmans, D., Emmons, L. K., Safieddine, S., Clerbaux, C., Edwards, D. P., & Coheur, P. F. (2016). Ozone variability in the troposphere and the stratosphere from the first 6 years of IASI observations (2008–2013). *Atmospheric Chemistry and Physics*, *16*(9), 5721–5743. https://doi.org/10.5194/acp-16-5721-2016

Wie, J., Moon, B.-K., Yeh, S.-W., Park, R. J., & Kim, B.-G. (2021). La Niña-related tropospheric column ozone enhancement over East Asia. *Atmospheric Environment*, *261*, 118575. https://doi.org/10.1016/j.atmosenv.2021.118575

Yang, S., Lau, K.-M., & Kim, K.-M. (2002). Variations of the East Asian Jet Stream and Asian–Pacific–American winter climate anomalies. *Journal of Climate*, *15*(3), 306–325. https://doi.org/10.1175/1520-0442(2002)015<0306:VOTEAJ>2.0.CO;2

Yang, Y., Li, M., Wang, H., Li, H., Wang, P., Li, K., et al. (2022). ENSO modulation of summertime tropospheric ozone over China. *Environmental Research Letters*, *17*(3), 034020. https://doi.org/10.1088/1748-9326/ac54cd